Int J Adv Manuf Technol (2015) 81:1757–1765
DOI 10.1007/s00170-015-7255-3

ORIGINAL ARTICLE

Effects of a ball-burnishing process assisted by vibrations in G10380 steel specimens

Jose Antonio Travieso-Rodriguez[1] · Giovanni Gomez-Gras[1] · Gilles Dessein[2] · Francisco Carrillo[2] · Joël Alexis[2] · Jordi Jorba-Peiro[3] · Nathalie Aubazac[2]

Received: 13 March 2015 / Accepted: 4 May 2015 / Published online: 27 May 2015

Abstract This paper explores the effects on the surface roughness, hardness and residual stress of G10380 steel specimens milled and treated with a ball-burnishing process assisted by vibrations. These vibrations are incorporated through the attachment of an induced coil module to a conventional burnishing tool, with forces transmitted through a pre-loaded spring. A positive effect of vibrations on the improvement and efficiency of the burnishing treatment is demonstrated, empirically proving that the vibrations introduce additional energy into the system that aids with displacements along the surface of the material to reallocate the crystalline structure. Significant results are found in terms of final surface roughness, which is highly improved in comparison to conventional burnishing treatments, even with fewer passes and a significant time reduction. Less robust results are observed in terms of specimen hardness and residual stress, but future improvements could be derived with a thorough development of the vibration system.

✉ Jose Antonio Travieso-Rodriguez
antonio.travieso@upc.edu

[1] Department of Mechanical Engineering, Universitat Politècnica de Catalunya, C. Comte d'Urgell, 187, Barcelona, Spain

[2] École Nationale d'Ingénieurs de Tarbes, 47 Avenue d'Azereix, Tarbes, France

[3] Department of Materials Science and Metallurgical Engineering, Universitat Politècnica de Catalunya, C. Comte d'Urgell, 187, Barcelona, Spain

Keywords Ball-burnishing · Vibrations · G10380 steel · Roughness · Residual stress · Hardness

1 Introduction

Metallic components for current industrial applications require high quality in terms of surface roughness and resistance levels to comply with demanding operational conditions. Mechanical components for machine tools, automobiles, aircrafts, moulds, conformation matrixes and many other industrial elements are composed of pieces that require high geometric tolerance and hardness levels, refined surface roughness and considerable mechanical resistance and surface integrity; they must also perform under stressful conditions, such as fatigue cycles.

Researchers are consistently developing new manufacturing systems in order to assure high-quality performance. Shepard et al. analysed the fatigue performance of Ti-6Al-4V parts for the aeronautical industry [1]. Surface roughness and compressive residual stresses were measured after performing fatigue studies on three pieces, each respectively finished with three different processes: burnishing, electropolishing and blasting. Although all three processes are considered to be highly effective, the ball-burnished parts showed the best results in surface roughness, with an average surface roughness of $R_a \approx 3\mu$m. The electropolished parts achieved an average surface roughness of 17μm, and the blasted parts were measured at 85μm. Burnishing can thus be positioned as the most refined finishing process.

Ball burnishing is a technological operation where surface irregularities are plastically deformed under the force of a pressing ball [2]. The process of plastic deformation of a material can be described through its stress-strain curve. Once the yield strength, which depends on the composition

and metallurgical state of the alloy, is exceeded, the material gradually deforms to a certain limit. This reference value is a function of several factors such as chemical composition, mechanical transformation processes or thermic treatments.

Nevertheless, some authors contend that ball burnishing has limits, particularly for surfaces where material hardness is too high to obtain optimal results because the required deformation forces cannot be obtained through the burnishing process. This fact supports the need to find new accessories and resources that could assist the burnishing process in order to widen its range of application and scope. Yinggang and Yung combined the burnishing process with a controlled laser beam that locally softened the surface of the pieces prior to burnishing [3]. Their experimental evidence showed better results in terms of surface roughness, higher compressive residual stresses and hardness in comparison to the conventional process.

Similar conclusions were drawn by Kozlov et al., who determined that yield strength could also be modified if the burnishing process was assisted in situ with vibration [4]. This phenomenon is known as acoustoplasticity [5] and occurs when a vibration acts in favour of the deforming force applied on the material, thus easing the reordering of the crystalline materials displacements. This is why the yield strength varies, thus requiring lower forces for material deformation.

Several commercial ball-burnishing tools currently exist, each using different functional mechanisms. For instance, Mahmood Hassan et al. and El-Axir et al. used ball-burnishing tools where the deforming force was transmitted through a spring [6, 7]. Other tools succeed in applying force with a hydraulic transmission system enabled by a closed circuit of pressurized fluid [8]. The latter can be acquired commercially from Mech-India Engineers Pvt. Ltd. [9] and Ecoroll AG Werkzeugtechnik [10].

Although all of the aforementioned tools generally improve the treated part (in terms of roughness, hardness and residual stress), most have yet to be improved with a complementary assisting mechanism and have been thus tested under conventional burnishing conditions. This study utilizes the vibration-assisted ball-burnishing (from now on, VABB) tool characterized by Gomez-Gras et al. [11]. The expectation of improved results for specimens treated with a VABB process, as compared to the traditional method, justify this study. In fact, no bibliographical reference can be found showing the results of this particular combination of tool and vibration assistance.

For the reasons stated above, this paper addresses the following questions:

1. Does the VABB improve the surface roughness values of the treated parts?
2. Does the VABB process increase workpiece hardness values compared to those obtained by the conventional burnishing process?
3. Does the VABB process vary the map of compressive residual stresses in the outer layers of the pieces by reaching higher values at deeper levels compared to those obtained with the ball-burnished conventional process?

The primary purpose and innovation of this paper is the study of properties obtained in pieces treated with VABB compared to those obtained in pieces treated with the conventional burnishing process in terms of surface roughness, hardness and residual stress.

The tool used for this study, as described in Spanish patent P20113033 [12], has the capacity to vibrate during the execution of the process as shown in Fig. 1a. For more details, Fig. 1b, c shows the attaching mechanism to the machine tool used to execute the treatment: a CNC machine where the piece has also been previously machined. The acting spring resides inside the tool body (Fig. 1a), resulting in a constant force during the ball-burnishing process.

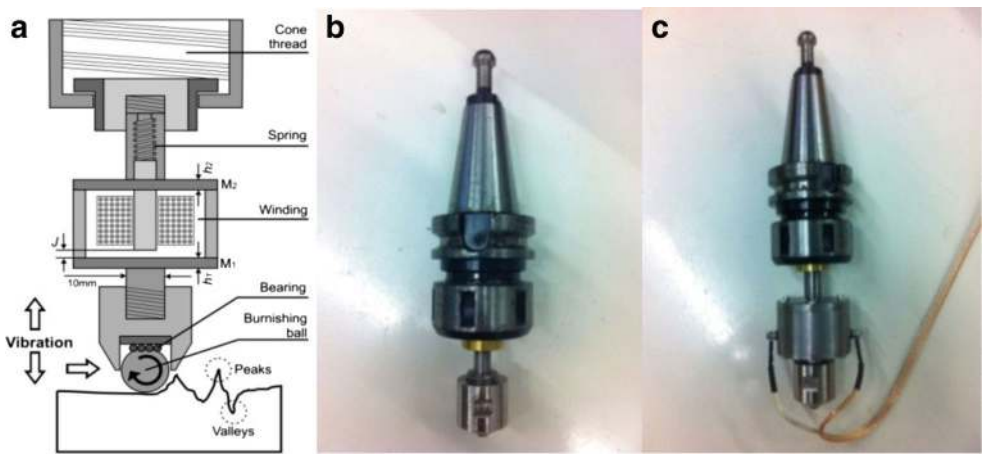

Fig. 1 Tools used in the experiments. **a** Functional diagram of the vibration system. M_1 Plate attached to the burnishing ball, M_2 plate attached to the spring, h_1:M_1 plate thickness, h_2: M_2 plate thickness, J gap. **b** Tool assembled for the non-vibration-assisted process. **c** Tool assembled for the vibration-assisted process. Parameter values: $h_1 = h_2 = 2$ mm, $J \leq 3$ mm [11]

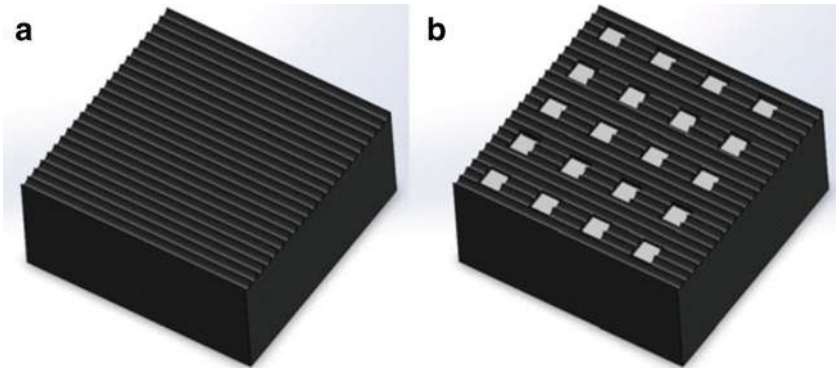

Fig. 2 Specimens used for testing the surface roughness. **a** 80 × 80 mm specimen after milling. **b** Subsequent state of the specimen, with 20 burnished 6 × 6 mm areas

An oscillatory force is added to this force, resulting in the vibration of the ball in reference to the treated surface. The vibration source is a magnetic field induced by a coil on a metal core. The coil is contained in a cylindrical tube, with two plates (M_1 and M_2) on its respective ends to close its volume. These plates vibrate jointly with the entire body of the tool and transmit that vibration to a burnishing ball with a 10-mm diameter. A spherical bearing, conformed by eight 2-mm-diameter spheres, allow the ball to advance in a free rotational movement. The entire tool is composed of several modules, although the vibrating module is detachable from the tool. This allows for the use of two different tools: one without vibration (Fig. 1b) and one with assisting vibrations (Fig. 1c). This tool is characterized in [11], and the frequency and amplitude of this vibration is defined in the following section.

The properties of materials used in the study and the different experiments undertaken are presented in Section 2. Subsequently, Section 3.3 explains the obtained results along with the information derived from them. Finally, the most important conclusions of this study are listed in Section 4.

2 Materials and methods

The objective specimens were made from heat treated and quenched G10380 steel with a hardness level of 150 HB. The procedure was performed by applying a force of 0.029 N for 10 s. These pieces were treated with both a VABB and conventional process, i.e., a non-vibration-assisted ball-burnishing process (NVABB). The shape and size of the workpieces are shown in Fig. 2. They were machined in a CNC milling machine with a mill of 8 mm in diameter at 3000 min^{-1} and at a feed rate of 1380 mm/min. They were subjected to a lateral pass width of 2 mm and a 0.5 mm depth of cut, thus obtaining two pieces of similar surface roughness [8]. The surface roughness values of the workpieces prior to burnishing can be found in the last row of Table 2 with the other roughness results. The subsequent burnishing operations were performed on both pieces, assisting the process with the vibration module on one and executing the conventional operation on the other.

Three parameters were evaluated during the burnishing operation: the burnishing force F (defined by the adjusted preload in the tool through the compression of the spring), the feed rate f and the number of burnishing passes n. In operations consisting of more than one pass, successive paths were always performed after previous ones.

The vibration regime of the VABB process was defined at 2637 Hz of frequency, which was the first natural frequency of the system; the amplitude was 1.3μm. Other processing parameters remained constant, i.e., a ball of hardened chromium steel (100Cr6) with a hardness value of approximately 57–66 HRC and a diameter of 10 mm, along with a lateral path width b of 0.08 mm. In addition, the burnishing strategy was consistent throughout the process, with the burnishing occurring at right angles with the previous milling operation. These parameters were sourced from testing conditions used in previous research literature [13].

Three measures were used to evaluate the quality of the piece after being subjected to the described process: surface roughness, hardness, and residual stress.

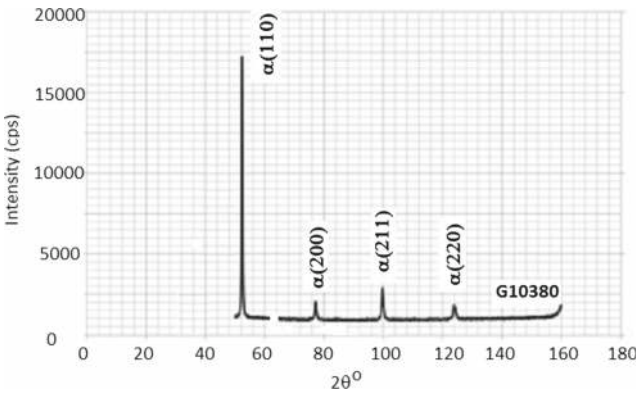

Fig. 3 X-ray diffraction spectrum of G10380 steel

Table 1 Measurement parameters for X-ray diffraction analysis

Material	X-ray radiation	Divergence slit	K_β filter	PSD scanning method	Number of ψ
G10380	Co = 1.78901 Å	Yes	Iron N	121° to 127°	750 min/φ

The roughness study was developed through 2^3 experimental designs resulting from combining different levels of the aforementioned parameters. This resulted in eight combinations with two replicates and four central points, thus producing a total of 20 different surfaces on each piece. Each burnishing operation was carried out either with or without vibrational assistance. Surface roughness was characterized by four indicators based on R_a (average surface roughness) and R_t (peak-valley maximal surface roughness), as well as in the parallel ($R_a \parallel$ and $R_t \parallel$) and perpendicular ($R_a \perp$ and $R_t \perp$) directions of the tool feed rate.

The hardness profile from the surface of the workpiece to its inner layers was evaluated to understand the effect of vibrations during the burnishing process on the superficial hardening of the material. Measures of hardness were executed on a surface right-angled to the burnished surface. The specimens were mounted in Bakelite and then ground and polished according to usual procedures for metallographic analysis. The Vickers Hardness was determined at five points on specimens burnished with and without vibrational assistance with a Buehler 5114 micro-hardness tester, applying a load of 0.029 N for 10 s. A 2-mm depth was tested starting from the burnished surface, and prints were adequately distributed to comply with ISO 6507 standards.

To evaluate the results of the process, residual stresses were estimated by X-ray diffraction in the milled regions and the regions treated with the ball burnishing process on each sample. The basic principle of this method measures strain to determine stress through the classical theory of elasticity. It consists of measuring interatomic d-spacings that are altered by elastic stresses. The stresses due to changes in interplanar spacing are determined by Eq. 1:

$$\sigma_\varphi = \left(\frac{d_\psi - d_{90^\circ}}{d_{90^\circ}}\right)\left(\frac{E}{1+\nu}\right)\frac{1}{\sin^2\psi} \quad (1)$$

In Eq. 1, E is the Young's modulus, ν is the Poisson coefficient, d_{90° and d_ψ are the interplanar spacings between planes that are parallel to the specimen surface and those at angles of ψ degrees, respectively. Taking into account Braggs law, Eq. 1 can be rewritten as Eq. 2:

$$\sigma_\varphi = \left(2\theta_{90^\circ} - 2\theta_\psi\right)\frac{\cot\theta}{2}\left(\frac{E}{1+\nu}\right)\frac{1}{\sin^2\psi} \quad (2)$$

The stresses were calculated for the highest possible diffraction angles in order to detect the small variations in the d-spacings and gain the best resolution for determining the residual stresses. The choice of radiation wavelength and the crystal plane family with the widest angle of diffraction length is important.

Diffraction analyses were performed with a Panalytical X Pert PRO diffractometer, and XRD analyses of various samples were performed with cobalt radiation (wavelength $\lambda_{k\alpha 1}$ = 1.7890100Å). A phase analysis of the materials was performed with a θ–2θ method to determine the crystal plane that diffracts with the highest angle in order to obtain the best resolution. Figure 3 shows the obtained diffractogram.

Residual stresses were determined from the variations of the distances between the crystal planes (220) of the centred cubic phase of α-ferrite that correspond to the highest angle of diffraction (2θ = 123.93°). All measurement conditions are shown in Table 1.

Changes in the diffraction angle θ as a function of the angle ψ are shown for the burnished steel with vibration in Fig. 4. We can trace the variation of the d-spacing based on $\sin^2\psi$ from these developments. The evolution of the d-spacing function to the $\sin^2\psi$ values is shown in Fig. 5. The stress can then be calculated from this plot by calculating the gradient of the line with basic knowledge of the elastic properties of the material. This approach assumes a zero stress at $d = d_{90^\circ}$, where d is the intercept on the y-axis

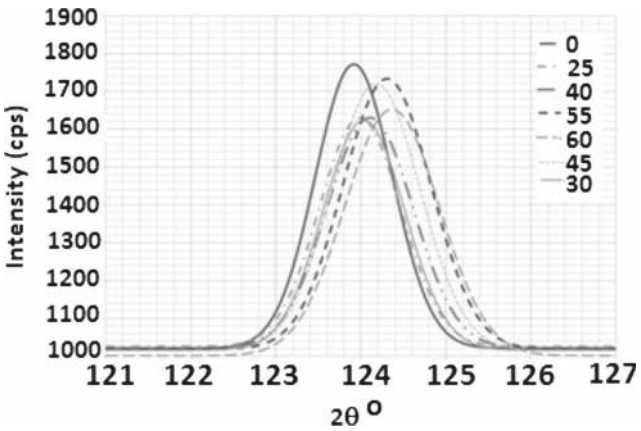

Fig. 4 Evolution of the diffraction angle 2 depending on the angles for the G10380 burnished samples with vibration

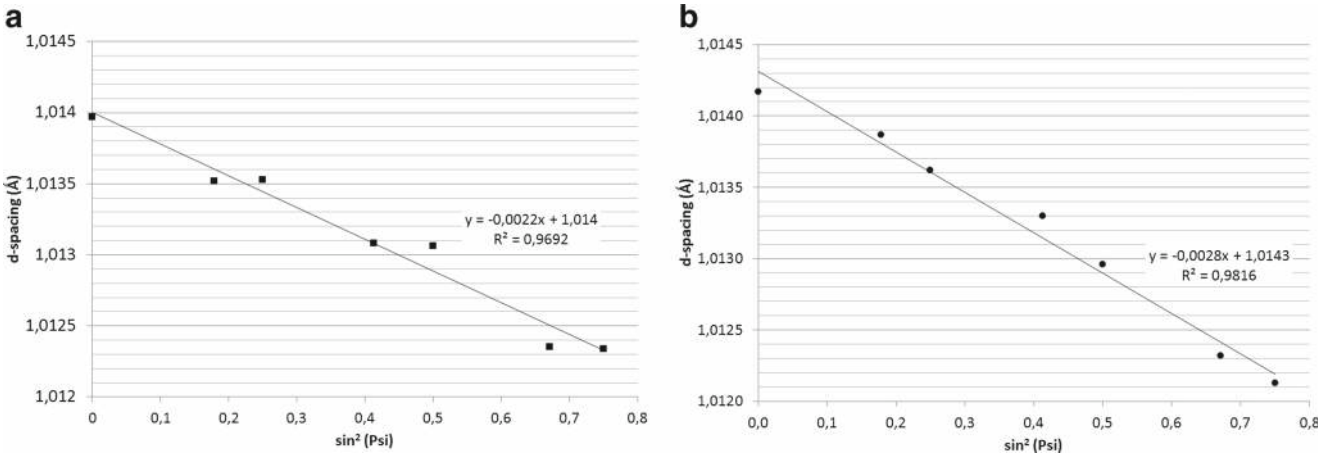

Fig. 5 Evolution of d-spacing based on $\sin^2\psi$ for the burnished G10380 samples. **a** NVABB. **b** VABB

when $\sin^2\psi = 0$. Given the high coefficient of determination of linear interpolations showing changes in lattice spacing versus $\sin^2\psi$, it can be seen that there is no influence of shear stresses on the surface or texture. Because the directional coefficient of the regression line is different in Fig. 5a, b, the residual stresses will be different according to the burnishing mode.

The elastic property values used for the stress calculation are $E = 222$ GPa and $\nu = 0.227$ for the crystal plane (220) [14]. To overcome the need to know the interatomic spacing without residual stress for each material, the results are given relative to residual stresses prior to burnishing. Residual stresses are determined for a given thickness, which is estimated at 30μm [15].

3 Results and discussion

3.1 Roughness measurement results

Table 2 shows the values of the measured surface roughness, which improved for all burnished specimens compared to specimens submitted to a previous milling operation without subsequent processing. The NVABB specimens experienced a 33 % improvement average in R_a along the parallel direction of the burnishing path and a 77 % improvement in the perpendicular direction. The VABB specimens experienced a decrease of R_a of 52 % in the parallel direction and 80 % in perpendicular measurements. In the case of R_t, the NVABB specimens experienced a 55 % improvement in the parallel direction of the burnishing path and a 58 % improvement in the perpendicular direction. In the VABB workpieces, this decreased by 65 % in the parallel direction and 60 % in perpendicular measurements (Table 2).

The process assisted by vibrations derived the best results in terms of roughness, considering the tested conditions. The $R_a \perp$ parameter was improved by 5 % and the $R_a \parallel$ parameter improved by 37 % on average. In the case of R_t, the parameters showed 5 and 10 % of improvement, respectively, with respect to burnishing without assistance.

Because the previous milling and the burnishing operations were performed at right angles, it is predictable that the differences between the roughness values obtained in different directions are dissimilar. Although the percentage results are discreet, it can be said that the VABB introduced improvements in the surface quality of the parts compared to those subjected to conventional burnishing.

Analyses were based on a Pareto chart, as shown in Fig. 6, where the most significant parameters were represented, taking into account a 95 % confidence level. More specifically, Fig. 6a shows the parameters that were significant after taking measurements of the average roughness R_a. It can be seen that the most important control variable was the deforming force, F, which was statistically significant in all measurements. The number of passes and their combination with the force had some relevance in these tests, but there was no clear trend in the results that allows for conclusions about these two parameters.

As for R_t, Fig. 6b shows the parameters that are significant after measuring, in all of the proposed conditions. The most important variable was also the force, F, which was statistically significant in all experiments. However, the number of passes n, as well as the combination of both, was also proven to be important in most cases. The feed, f, was not relevant in any of the conditions studied, as occurred in measurements of R_a. For this reason, it has not been represented in Fig. 6.

Table 2 Results of surface roughness measurements (μm)

				NVABB				VABB			
Experiment	F (N)	f (mm/min)	Number	$R_a \perp$	$R_t \perp$	$R_a \parallel$	$R_t \parallel$	$R_a \perp$	$R_t \perp$	$R_a \parallel$	$R_t \parallel$
1	130	600	1	1.22	1.05	3.90	11.19	0.40	7.40	2.21	7.51
2	120	600	5	1.14	2.92	3.82	9.69	0.47	4.13	3.13	10.03
3	130	400	1	1.22	8.44	4.26	10.87	0.20	4.50	3.02	10.20
4	125	500	3	1.14	4.83	3.47	8.01	0.48	3.78	1.67	8.79
5	125	500	3	1.16	6.75	3.45	7.06	0.79	4.33	1.93	9.42
6	125	500	3	1.15	6.74	3.74	9.74	0.40	3.73	2.22	6.14
7	120	600	1	1.18	5.81	3.99	11.83	1.08	7.96	3.57	8.16
8	130	400	5	1.18	3.03	2.12	9.02	0.16	2.50	1.62	7.75
9	130	400	1	1.21	7.02	2.81	6.09	0.17	5.27	3.58	6.05
10	125	500	3	1.18	3.86	3.47	10.38	0.62	4.44	2.75	8.53
11	130	600	5	1.16	9.06	2.61	8.58	0.70	3.77	0.91	5.14
12	120	600	1	1.17	6.15	4.33	12.14	0.74	7.59	4.31	9.78
13	130	600	1	1.25	5.18	2.87	8.58	0.68	7.55	2.45	9.28
14	120	400	5	1.14	7.87	3.51	7.83	0.46	3.01	2.94	13.00
15	120	400	5	1.13	8.92	3.03	9.70	0.40	2.49	2.83	8.79
16	120	600	5	1.14	10.91	3.82	7.59	0.30	3.35	2.76	7.98
17	120	400	1	1.18	10.95	4.40	8.10	0.59	6.68	3.34	7.54
18	130	400	5	1.18	8.18	2.25	9.41	0.16	3.35	2.11	8.88
19	130	600	5	1.15	5.96	2.69	10.38	0.41	3.51	1.47	7.33
20	120	400	1	1.18	7.89	3.87	6.59	0.47	6.59	3.33	8.36
Previous milling				4.03	16.21	5.08	20.26	3.32	13.59	5.66	19.75

The average roughness was further studied to determine its relevance as the most representative measure of the surface quality of a workpiece. For this purpose, a comparative analysis of the influence of the combination of processing parameters (f, F and n) on the final R_a was performed. Similar results were obtained for one pass when using vibration-assisted burnishing and five passes without the vibrations assistance. Performing the procedure in one

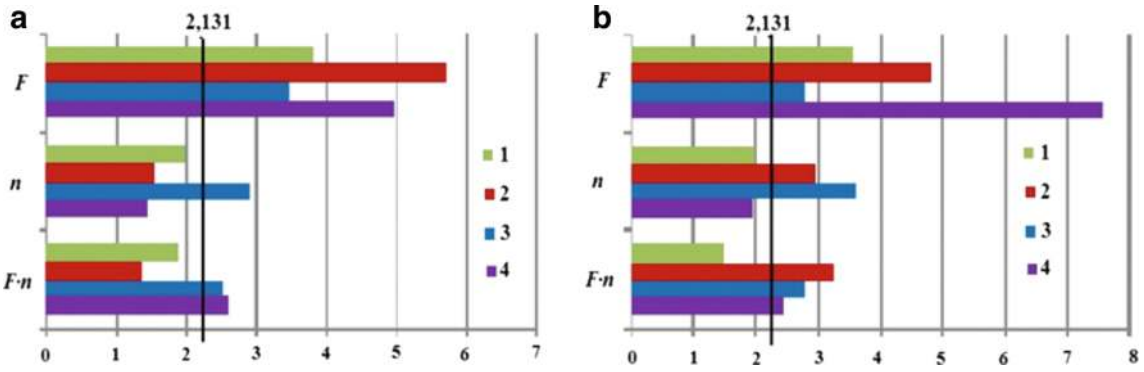

Fig. 6 Pareto chart for standardized effects of the different system variables. **a** *1* NVABB $R_a \perp$, *2* NVABB $R_a \parallel$, *3* VABB $R_a \perp$, *4* VABB $R_a \parallel$. **b** *1* NVABB $R_t \perp$, *2* NVABB $R_t \parallel$, *3* VABB $R_t \perp$, *4* VABB $R_a \parallel$

pass is desirable and would save a considerable amount of time. This can be seen in results presented in Table 2.

In addition, burnishing in just one pass with vibrational assistance significantly decreases the dispersion of measured values. Changes in the feed of the tool in its values do not substantially affect the value of dispersion and roughness. Therefore, burnishing with a 600-mm/min feed is desirable to reduce processing time and increase efficiency.

In addition, burnishing with just one pass with assitance of vibrations significantly decreases the dispersion of measured values. Changing in the feed values of the tool does not substantially affect the value of dispersion and roughness. Therefore, burnishing with a 600-mm/min feed is desirable to reduce processing time and increase efficiency.

3.2 Measured superficial hardness results

Figure 7 summarizes the values associated to each of the performed operations. The results were calculated as the average value of at least ten different measurements for each test. The total measurement error is the result of the sum of the precision error of the measurements plus the durometer target error plus the statistical error.

Working with forces of 100 N increases the hardness compared to 90 N while keeping the remaining variables constant (Fig. 7a). Although the increase is not high, the difference is noticeable. The small variation in the forces is only considerable in the outermost layers between 10 and 50 μm, where the hardening becomes more visible. In deeper layers, the difference of 10 N does not appear to have a significant effect.

However, in the experiments performed at the maximum number of passes and forces, the difference between the VABB and NVABB approaches are considerable (Fig. 7b & d). At the 80–100 μm depth, the hardening is noticeable, but at deeper layers, little variation can be corroborated. This means that the assistance of vibration can only increase hardness at a superficial layer; this aid does not reach significant depths.

Based on the number of passes, it can be said that the differences are not relevant between performing VABB in five passes or just one. Further hardening only occurs to a depth of 50 μm (Fig. 7c). Although the experimental results are enlightening, it would be interesting to determine how many passes would be required for the steel under study to reach the maximum capacity of self-hardening by deformation.

Regardless of the small variations already discussed, the increase in hardness generally reaches a maximum value

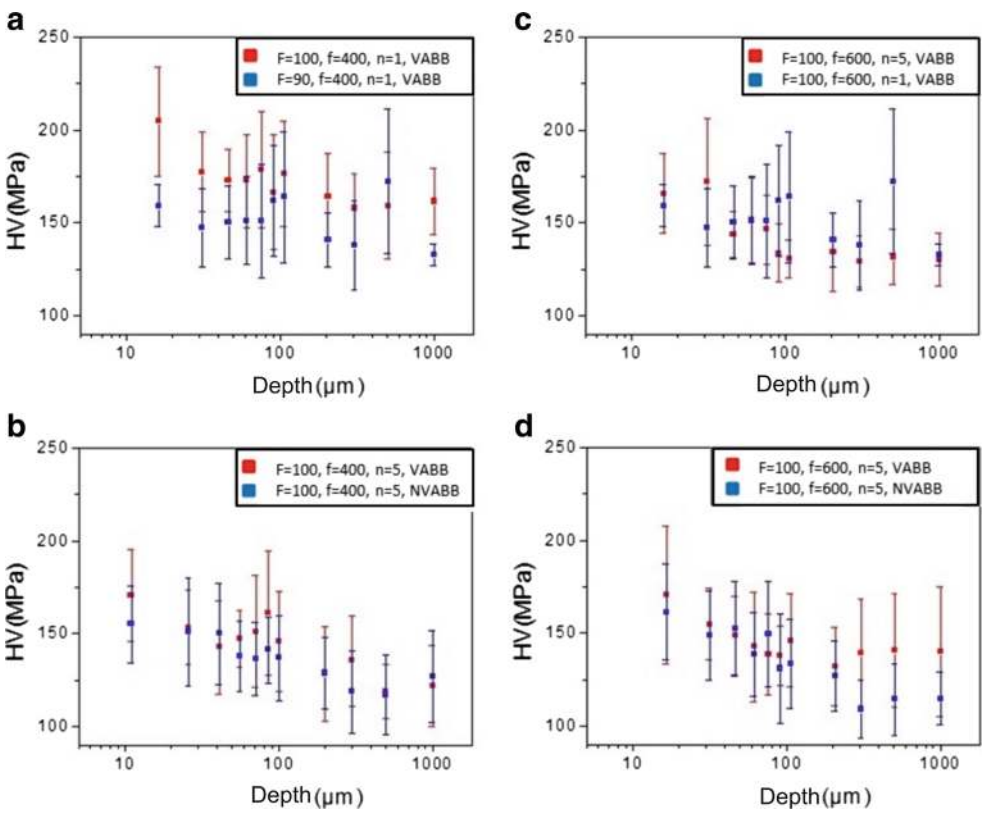

Fig. 7 Measured micro-hardness profile (load HV0.003) of the specimen obtained with burnishing forces $F_1 = 100$ N and $F_2 = 90$ N and **a** $f = 400$ mm/min and $n = 1$ with vibrations, **b** $f = 400$ mm/min and $n = 5$, with vibrations and without them, **c** $f = 600$ mm/min and $n = 5$ with vibrations and **d** $f = 600$ mm/min and $n = 5$, with vibration and without them

Table 3 Results of residual stress on steel samples

			Sample 1—NVABB		Sample 2—VABB	
Exp.	F (N)	Number	Measured valour [MPa]	Improvement [MPa]	Measured valour [MPa]	Improvement [MPa]
1	110	1	−384	171	−485	205
2	100	1	−440	227	−545	265
3	110	3	−451	238	−551	271
4	100	3	−443	230	−535	255
Before burnishing			−213		−280	

at a depth of approximately 100 μm. In percentages, the increase in micro-hardness for NVABB is approximately 4 % with conventional ball-burnishing and 5 % using the VABB process. Despite these modest results, it can be said that the VABB does increase the surface hardness of pieces for the tested conditions.

Assisting the ball-burnishing process with vibrations enhances the forces acting in the system, thus making the treatment more feasible. This phenomenon was explained by Yin and Shuinmura [16]. However, burnishing at the working frequency of the tool (approximately 2600 Hz) adds no significant forces to the process. The values of the forces were measured by placing the workpieces on a Kistler model 9257B dynamometer and monitored in real time to record the force values applied in all of the experiments. The sampling frequency was 10 KHz, and data were obtained for 1 min during the experiment. The forces applied in both the VABB and NVABB processes differed in a range of 5 to 8 N for all experiments. The increase of applied forces in the VABB operations had a certain influence on the surface roughness, as already stated. However, the hardness values did not vary considerably, probably because this extra applied force was insufficient.

The action of the vibration waves dissipated power that helped release the dislocations present in the outermost layers of the material, as was explained by Holstein in 1959 [17]. The most relevant consequence is that, by introducing vibrations into the process, the same results can be obtained faster and more easily. This explains why the results obtained with one pass of the VABB process were the same as with five passes of the non-assisted burnishing.

3.3 Residual stress results

The values of compressive residual stress, as estimated by X-ray diffraction, increased in the burnished areas of the workpieces in comparison to the milled surfaces (Table 3). This was a common effect for both conventional ball-burnishing (where the increases were approximately 216 MPa on average) and the VABB process (where the increases were approximately 249 MPa on average). Therefore, burnishing assisted by vibration results in higher values of compressive residual stresses.

However, when a force of 110 N and three passes were used for the burnishing operation, the residual stress values obtained were higher as expected. Although these values were different compared to the only-milled specimens, there was no significant difference between residual stresses after submitting the specimen to both burnishing operations. These results suggest that the initial residual stress distribution did not significantly affect the residual stress produced by the ball-burnishing, thus corroborating the conclusions reached by Roettger [18].

Similar experiments and results have been obtained and analysed for aluminium alloy A92017 in Travieso-Rodriguez et al. [19].

4 Conclusions

The results obtained after the performed operations and tests support the hypothesis assumed at the beginning of this paper, i.e., when pieces of G10380 steel are treated with a VABB process, their properties are superior to those obtained when the steel is treated with conventional ball-burnishing. More specifically, the following can be stated:

1. Surface roughness parameters, R_a and R_t, are improved when the burnishing treatment of the objective workpieces is assisted by vibrations.
2. The assistance of the burnishing process by vibrations results in fewer required burnishing passes to

improve surface roughness. Therefore, the processing time decreases for the range of parameters used in this paper.

3. The hardness in the workpiece profiles increases when assisting the burnishing process with vibrations; while noticeable, the levels are not significant with the parameters used in these experiments.
4. As expected, the conclusions described for hardness are also applicable for the residual stresses.

Acknowledgments This paper was written in collaboration with the TECNOFAB group from EUETIB-UPC (Spain) and the Laboratoire Gnie de Production (LGP) from ENIT (France). Financial support for this study was provided by the Ministry of Economy and Competitiveness in Spain through grant DPI2011-26326 (J-01686) and is greatly appreciated.

References

1. Shepard MJ, Prevey PS, Jayaraman N (2003) Effects of surface treatment on fretting fatigue performance of Ti-6Al-4V. In: Proceedings of the 8th national turbine engine high cycle fatigue (HCF) Conference, April 14-16, Monterrey, CA
2. Travieso-Rodriguez JA, Dessein G, Gonzalez-Rojas HA (2011) Improving the surface finish of concave and convex surfaces using a ball burnishing process. Mater Manuf Process 26(12):1494–1502
3. Yinggang T, Yung CS (2007) Laser-assisted burnishing of metals. Int J Mach Tools Manuf 47:14–22
4. Kozlov AV, Mordyuk AV, Chernyasshevsky AV (1995) On the additivity of acoustoplastic and electroplastic effects. Mater Sci Eng 190(1-2):75–79
5. Siua KW, Ngana HW, Jones IP (2011) New insight on acoustoplasticity-ultrasonic irradiation enhances subgrain formation during deformation. Int J Plast 27(5):788–800
6. Mahmood HA (2008) The effects of ball- and roller-burnishing on the surface roughness and hardness of some non-ferrous metals. J Mater Process Technol 72(5):385–391
7. El-Axir MH, Othman OM, Abodiena AM (2008) Study on the inner surface finishing of aluminium alloy 2014 by ball-burnishing process. J Mater Process Technol 202:435–442
8. Travieso-Rodriguez JA (2010) Estudio para la mejora del acabado superficial de superficies complejas, aplicando un proceso de deformacin plstica (bruñido con bola). PhD Thesis. Universitat Politecnica de Catalunya, Barcelona (Spain)
9. Mech-India Engineers Pvt. Ltd. Retrieved from http://www.mechindia.com/. Last visited on 24/11/2014
10. Ecoroll AG Werkzeugtechnik hydrostatic tools catalogue. Retrieved from http://www.ecoroll.de/en/products/hydrostatische-werkzeuge.html. Last visited on 24/11/2014
11. Gomez-Gras G, Travieso-Rodriguez JA, Gonzalez-Rojas HA, Napoles-Alberro A, Carrillo F, Dessein G (2014) Study of a ball-burnishing vibration-assisted process. In: Proceedings of the Institution of Mechanical Engineers, Part B: Journal of Engineering Manufacture, vol 229, no 1, pp 172–177. doi:10.1177/0954405414526383
12. Travieso-Rogdriguez JA, Gonzalez-Rojas HA, Casado-Lopez R (2013) Herramienta con bola a baja presin, aplicable para bruido de superficies. Spanish patent reference: P201130331. Boletín Oficial de la Propiedad Intelectual BOPI
13. Holstein T (1959) Theory of ultrasonic absorption in metals: the collision-drag effect. Phys Rev 113(2):479–496
14. Rodriguez A, Lopez de la Calle LN, Celaya A, Lamikiz A, Albizuri J (2012) Surface improvement of shafts by the deep ball-burnishing technique. Surface and Coatings Technology 206:2817–2824
15. Luca L (2002) Investigation into the use of ball burnishing of hardened steel components as a finishing process. PhD Dissertation, University of Toledo (USA)
16. Fangjung S, Chienhua C (2003) Freeform surface finish of plastic injection mould by using ball-burnishing process. J Mater Process Technol 140:248–254
17. Yin S, Shuinmura T (2004) A comparative study: polishing characteristics and its mechanisms of three vibration modes in vibration-assisted magnetic abrasive polishing. Int J Mach Tools Manuf 44:383–390
18. Roettger K (2002) Walzen hartgedrehter Oberflaechen. PhD Dissertation, RWTH Aachen University (Germany)
19. Travieso-Rodriguez JA, Gomez-Gras G, Jorba-Peiro J, Carrillo F, Dessein G, Alexis J, Gonzalez-Rojas H (2015) Experimental study on the mechanical effects of the vibration-assisted ball-burnishing process. Mater Manuf Process. first published on April 2015. doi:10.1080/10426914.2015.1019114